IGARSS 2022 - 2022 IEEE International Geoscience and Remote Sensing Symposium | 978-1-6654-2792-0/22/$31.00 ©2022 IEEE | DOI: 10.1109/IGARSS46834.2022.9884759

LEAF NITROGEN ASSESSMENT WITH ISS DESIS IMAGING SPECTROMETER AS COMPARED TO HIGH-RESOLUTION AIRBORNE HYPERSPECTRAL IMAGERY

*Y. Wang [1, *], L. Suarez [1, 2], V. Gonzalez-Dugo [3], D. Ryu [1], P. Moar [4], P.J. Zarco-Tejada [1, 2, 3]*
** E-mail address: wang.y@unimelb.edu.au*

[1] Department of Infrastructure Engineering, Faculty of Engineering and Information Technology (FEIT), University of Melbourne, Melbourne, VIC 3010, Australia
[2] School of Agriculture and Food, Faculty of Veterinary and Agricultural Sciences (FVAS), University of Melbourne, Melbourne, VIC 3010, Australia
[3] Instituto de Agricultura Sostenible (IAS), Consejo Superior de Investigaciones Cientificas (CSIC), Avenida Menendez Pidal s/n, 14004 Cordoba, Spain
[4] College of Science, Health and Engineering, School of Engineering and Mathematical Sciences, La Trobe University, Victoria 3086, Australia

ABSTRACT

Traditional methods to estimate leaf nitrogen (N) from satellite imagery rely on structural and chlorophyll *a*+*b* (C_{ab}) vegetation indices. Recent progress with airborne hyperspectral imagery identified C_{ab} and SIF as critical indicators for evaluating leaf N variability, yielding superior performance than standard vegetation indices. In tree orchards, accurate physiological assessments require high-spatial-resolution hyperspectral imagery to minimize canopy architecture and soil background effects. Understanding the potential of coarse-spatial-resolution spaceborne hyperspectral imagery for leaf N estimation is critical. In this study, DESIS hyperspectral imagery collected on board the International Space Station was used to assess the quantification of leaf N, evaluating the relative contributions of physiological plant traits and SIF. High-resolution airborne hyperspectral imagery and ground N data were used for validation. Results show that C_{ab} and SIF were the most critical parameters explaining leaf N both from DESIS and from airborne hyperspectral imagery, yielding strong correlations against ground truth N data (r^2=0.90, p<0.0001) and with airborne-predicted N (r^2=0.75, p<0.0001).

Index Terms – DESIS, Nitrogen, Hyperspectral, Spaceborne, Almond, Chlorophyll, SIF, Plant traits

1. INTRODUCTION

Accurate leaf nitrogen (N) assessment is crucial for ensuring adequate nutrient levels and determining fertilizer requirements over the course of the growing season. Monitoring leaf N status at large scales requires remote sensing technologies to achieve affordable quantifications compared with traditional biochemical analyses of leaf tissues. Standard remote sensing methods for N assessment typically use structural and chlorophyll-sensitive vegetation indices derived from multispectral sensors, but relationships saturate at high N levels [1]. Spaceborne hyperspectral sensors can measure detailed spectral features over large areas. The German Aerospace Center (DLR) Earth Sensing Imaging Spectrometer (DESIS) onboard the International Space Station (ISS) is capable of collecting hyperspectral imagery from space. However, leaf N assessment in row-structured orchards is affected by the canopy architecture and background. Thus, the implications of using coarser spatial resolution hyperspectral imagery on the accuracy of N estimation in heterogeneous orchards are crucial.

Previous work [2, 3] on the assessment of leaf N from airborne hyperspectral imagery demonstrated that Solar-Induced Fluorescence (SIF) and physiological plant traits (i.e., C_{ab} and other leaf biochemicals) retrieved from radiative transfer models (RTM) yielded superior N estimates than standard vegetation indices. These methods showed that C_{ab} and SIF predicted 95% of the N variability in almond orchards. However, the importance of specific plant traits may differ considerably at coarser spatial resolution due to the structural and background effects. This study investigates the contribution of SIF and the leaf biochemistry quantified by RTM inversions from ISS DESIS hyperspectral imagery for large-scale N assessment in almond orchards, with comparison against high-resolution airborne hyperspectral imagery and ground truth data used as validation.

2. MATERIALS AND METHODS

2.1. Study area

The study site is a commercial almond orchard covering about 1,200 hectares, located in northwestern Victoria,

Australia. Three different almond varieties were alternately planted in groups of 6 rows for cross-pollination [4] in 2006 and 2007, comprising Nonpareil (50%), Carmel (33%), and Price (17%). Plant varieties are spaced apart by 7 m and trees by 4.4 m, respectively. Nutrients were supplied to plants via drip fertigation and separated by one-hour intervals between varieties. During the 2020-2021 growing season, the fertigation rate for Nonpareil was 10% lower than that of Carmel and Price throughout the orchard.

2.2. Datasets

2.2.1. Field measurements

The field measurements and leaf sampling were conducted at the pre-harvest stage on February 1, 2021 in 13 homogeneous study plots throughout the orchard. A total of eighty fully exposed leaves of Nonpareil and Carmel were collected and measured from each study plot by different handheld instruments, including leaf C_{ab}, anthocyanins (Anth), flavonol content and the nitrogen balance index (NBI) using a Dualex-4 Scientific instrument (FORCE-A, Orsay, France), steady-state leaf chlorophyll fluorescence (Ft) with a FluorPen FP 110 (PSI, Brno, Czech Republic), and leaf reflectance spectra over the visible and NIR regions with a PolyPen RP 400 instrument (PSI, Brno, Czech Republic). Moreover, ten additional leaves per variety (a total of 100 leaf samples per plot) were collected for N determination in the biochemical laboratory using the Dumas Combustion method [5] with a LECO Nitrogen Analyzer (LECO Corporation, MI, USA).

2.2.2. Airborne hyperspectral imagery

An airborne campaign was carried out at solar noon under clear sky conditions on January 31, 2021. A hyperspectral line-scanning sensor (Micro-Hyperspec VNIR model, Headwall Photonics, Fitchburg, MA, USA), covering 371 bands from the visible and the near-infrared regions with an FWHM of 5.8nm and a spectral sampling interval of 1.6 nm, was flown onboard the Cessna 172R aircraft operated by the HyperSens Laboratory, the Airborne Remote Sensing facility of The University of Melbourne. The imagery was collected at 550 m above ground level with a spatial resolution of 40 cm. Pre-processing and calibration steps of the raw images were performed as described in Zarco-Tejada et al. [6]. The high-spatial resolution of the airborne hyperspectral imagery enabled the extraction of sunlit vegetation pixels to quantify leaf biochemistry and SIF [2]. In a two-year validation study conducted for the entire orchard, leaf N (r^2=0.95, p<0.001, Figure 1) was estimated with C_{ab} and SIF being the most critical plant traits [3].

2.2.3. DESIS hyperspectral imagery acquired from the ISS

A 30-meter spacebore hyperspectral scene was captured by the DESIS imaging spectrometer onboard the ISS on January 23, 2021. The imagery covers 235 spectral bands, ranging from the visible to the near-infrared regions with a 3.5 nm

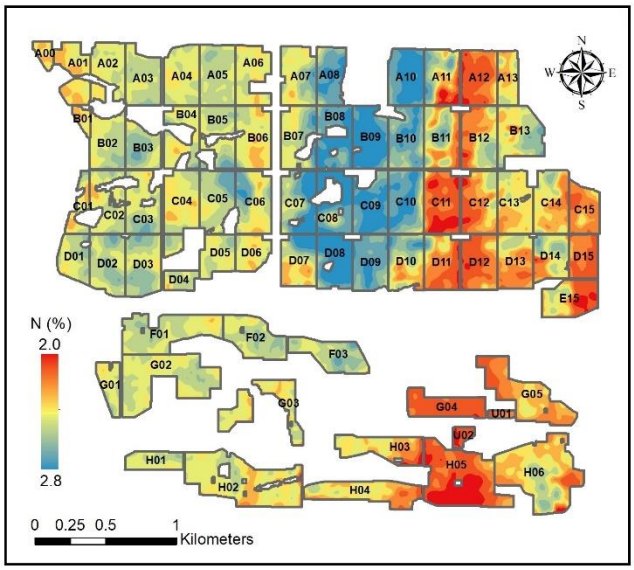

Figure 1. Airborne predicted N map derived from C_{ab} and SIF at a 1,200-ha almond orchard study site in Victoria, Australia.

FWHM and a 2.55 nm sampling interval [7]. As a result of the signal noise in the blue and green spectral regions, additional cross-calibration was performed for DESIS L2A imagery using vegetation, soil and water features from airborne hyperspectral imagery by 3×3 DESIS pixel windows (Figure 2).

2.3. Plant traits retrievals and SIF quantification

The reflectance spectra of individual vegetation pixels were extracted for the calculation of structural and chlorophyll indices (e.g., NDVI, EVI, TCARI/OSAVI), as well as plant traits (e.g., C_{ab}, carotenoids (C_{car}), Anth, the de-epoxidation state of the xanthophyll-cycle pigments (C_x), dry matter (C_{dm}) and leaf area index (LAI)) retrieval from FluSAIL RTM [8, 9]. An artificial neural network model [10] based on a look-up-table (LUT) with random 50,000 simulations was used to retrieve the physiological plant traits.

The Fraunhofer Line Depth (FLD) principle [11] was used to calculate SIF using the O_2-A oxygen absorption feature from the DESIS L1C radiance imagery. Irradiance data were derived from auxiliary data collected at the nearest station on the day of DESIS overpass. The same method was applied to the airborne hyperspectral imagery to retrieve SIF and the plant traits by RTM inversions.

2.4. Statistical analysis for nitrogen estimation

The statistical methods used to assess N from airborne imagery [2, 3] were applied in this study to DESIS data. The variance inflation factor (VIF) collinearity assessment and the out-of-bag (OOB) predictor importance were also determined for DESIS. We compared the relative contributions of physiological plant traits (i.e., C_{ab}, C_{car}, Anth,

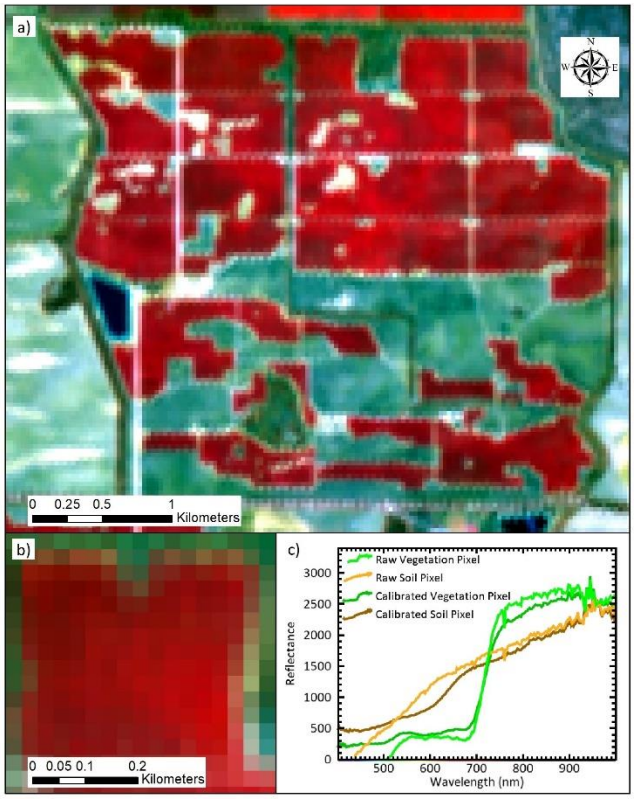

Figure 2. a) False colour composite of DESIS hyperspectral imagery over a 1,200-ha almond orchard, b) DESIS zoom-in view over the planting blocks, and c) reflectance spectra from raw L2A image and cross-calibrated DESIS imagery.

C_x, C_{dm}, LAI) and SIF to estimate leaf N between spaceborne DESIS hyperspectral and airborne hyperspectral imagery throughout the almond orchard. The leaf N estimates obtained from random forest regression models using DESIS were validated with field measured leaf N and the high-resolution airborne hyperspectral-based retrievals.

3. RESULTS

The traditional structural indices (e.g., NDVI, MCARI1) calculated from DESIS hyperspectral imagery were strongly related to C_{ab}, but yielded a weak relationship with N (Table 1). NDVI yielded r^2=0.35 (p<0.05) with leaf measured C_{ab}, but was unable to explain N when compared either against laboratory N measurements (r^2=0.08, n.s.) or the airborne-based N validation map (r^2=0, n.s.). These results suggest that the variability of the canopy architecture captured at the spaceborne scale did not explain leaf N orchard variability. Other traditional chlorophyll indices (e.g., TCARI/OSAVI) used for N assessment did not correlate with leaf C_{ab} nor N from DESIS data, likely due to the mixture of soil and shaded canopy components captured at such spatial resolution. Nevertheless, CTRI1 [12] exhibited a significant correlation with leaf N (r^2=0.45, p<0.05) and with the airborne-predicted N (r^2=0.74, p<0.01), outperforming other vegetation indices.

SIF quantified from DESIS showed statistically significant relationships with field measured Ft (r^2=0.52, p<0.01) (data not shown), leaf C_{ab} (r^2=0.62, p<0.01) and with leaf N (r^2=0.56, p<0.01).

Table 1. Coefficients of determination (r^2) for the DESIS vegetation indices against field measurements and N derived from the airborne hyperspectral imagery.

Vegetation index	Leaf C_{ab}	Leaf PRI	Leaf N (%)	Airborne predicted N (%)
NDVI	0.35**	0.06	0.08	0
EVI	0.65***	0.24*	0.31**	0.20
MCARI1	0.69***	0.29*	0.35**	0.27*
SRPI	0.01	0.26	0.18	0.33**
TCARI/OSAVI	0.06	0.19	0.20	0.03
CTRI1	0.20	0.47***	0.45**	0.74***
SIF	0.62***	0.62***	0.56***	0.67***

*p < 0.1, **p < 0.05, ***p < 0.01

As illustrated in Table 2, C_{ab} retrieved by RTM showed greater correlations with leaf C_{ab} (r^2=0.31, p<0.1), leaf N (r^2=0.63, p<0.01) and airborne-predicted N (r^2=0.80, p<0.01) than chlorophyll indices. In addition to C_{ab}, other plant traits such as C_x (r^2=0.71, p<0.01) were also strongly correlated with leaf N. Significant relationships were also observed between retrieved leaf pigments (i.e., C_{ab}, C_{car}, C_x) and SIF (e.g., C_{ab}, r^2=0.59, p<0.01). In contrast to biochemical plant traits, the structural trait LAI did not yield a significant relationship with leaf C_{ab} nor N at DESIS scale.

Table 2. Coefficients of determination (r^2) among RTM-derived plant traits from DESIS and field measurements, canopy SIF and N derived from the airborne hyperspectral imagery.

Estimated parameter	Leaf C_{ab}	SIF	Leaf N (%)	Airborne predicted N (%)
C_{ab} (µg/cm²)	0.31*	0.59***	0.63***	0.80***
C_{car} (µg/cm²)	0.07	0.32**	0.17	0.14
Anth (µg/cm²)	0.10	0.01	0.03	0.16
C_x	0.26*	0.41**	0.71***	0.38**
C_{dm} (g/cm²)	0.07	0.12	0.37**	0.27*
LAI	0.14	0.22	0.07	0.01

*p < 0.1, **p < 0.05, ***p < 0.01

The relative contribution of each plant trait to leaf N estimation from spaceborne DESIS and airborne scales appeared to be highly consistent (Figure 3). These results identified C_{ab}, SIF, and C_x as the most critical spectral traits when explaining N variability, followed by the rest of the retrieved biochemical constituents and biophysical traits. Furthermore, the statistical analysis revealed that C_{ab} and SIF were non-collinear (VIF<5) but other biochemical constituents (i.e., C_x, C_{car} and C_{dm}) showed higher collinearity with C_{ab}. These collinear traits were dropped from the final model to reduce redundancy. Consequently, a

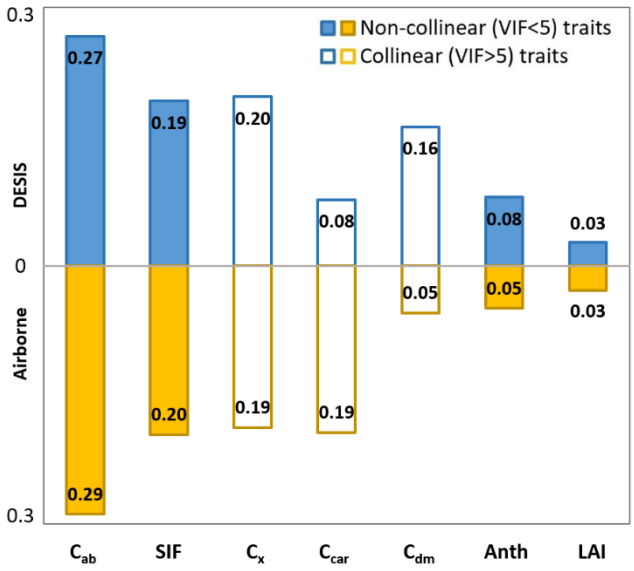

Figure 3. Relative contribution of FluSAIL RTM-inverted plant traits and SIF on the N prediction models from DESIS and airborne hyperspectral imagery.

model consisting of C_{ab} and SIF together yielded r^2=0.90 (p<0.0001) against leaf N, and r^2=0.75 (p<0.0001) against airborne-predicted N in the almond orchard comprising different varieties, ages, and planting structures.

4. CONCLUSIONS

Results shown in this study demonstrate that RTM-derived plant traits and SIF retrieved from DESIS hyperspectral imager onboard the International Space Station yielded strong relationships with ground leaf N and with estimatd N carried out from high-resolution airborne hyperspectral imagery. The most critical parameters explaining N from DESIS in this study agreed with those derived from the airborne hyperspectral imagery. Accordingly, the estimated C_{ab} retrieved by RTM inversion and SIF made a greater contribution to explaining leaf N than the rest of the biochemical constituents and biophysical traits, both from DESIS and airborne hyperspectral imagery. C_{ab} and SIF predicted 90% of the leaf N variability found in the almond orchard, obtaining a 75% agreement with the high-resolution airborne N estimates. The present study confirms the importance of the coupled C_{ab} and SIF for leaf N assessment in tree orchards at the spaceborne scale, demonstrating the feasibility of large-scale leaf N quantification for precision agriculture purposes.

5. ACKNOWLEDGMENTS

We are grateful to McPherson Family and Invergowrie Foundation for the financial support and the assistant from the Mallee Regional Innovation Centre (MRIC). Special thanks to Xiaojin Qian and Tomas Poblete from HyperSens Remote Sensing Laboratory for their support during the field and airborne campaigns. We acknowledge German Aerospace Center (DLR) for accessing DESIS data and Brian Slater for allowing this research to be carried out in Aroona Farms. We also thank Rafael Romero, David Notario and Alberto Hornero from QuantaLab IAS-CSIC (Spain) for laboratory support.

6. REFERENCES

[1] M. Schlemmer *et al.*, "Remote estimation of nitrogen and chlorophyll contents in maize at leaf and canopy levels," *International Journal of Applied Earth Observation and Geoinformation,* vol. 25, pp. 47-54, 2013.

[2] Y. Wang *et al.*, "Assessing the Contribution of Airborne-Retrieved Chlorophyll Fluorescence for Nitrogen Assessment in Almond Orchards," in *2021 IEEE International Geoscience and Remote Sensing Symposium IGARSS*, 2021: IEEE, pp. 5853-5856.

[3] Y. Wang, L. Suarez, T. Poblete, V. Gonzalez-Dugo, D. Ryu, and P. Zarco-Tejada, "Evaluating the role of solar-induced fluorescence (SIF) and plant physiological traits for leaf nitrogen assessment in almond using airborne hyperspectral imagery," *Remote Sensing of Environment,* In Review.

[4] W. Asai, W. Micke, D. Kester, and D. Rough, "The evaluation and selection of current varieties," *Almond production manual,* pp. 52-60, 1996.

[5] J. B. A. Dumas, "Procedes de l'analyse Organic," *Annales de Chimie et de Physique (Annals of Chemistry and of Physics),* vol. 247, pp. 198-213, 1831.

[6] P. Zarco-Tejada *et al.*, "Previsual symptoms of Xylella fastidiosa infection revealed in spectral plant-trait alterations," *Nature Plants,* vol. 4, no. 7, pp. 432-439, 2018.

[7] A. Eckardt *et al.*, "Desis (dlr earth sensing imaging spectrometer for the iss-muses platform)," in *2015 IEEE international geoscience and remote sensing symposium (IGARSS)*, 2015: IEEE, pp. 1457-1459.

[8] N. Vilfan *et al.*, "Extending Fluspect to simulate xanthophyll driven leaf reflectance dynamics," *Remote sensing of environment,* vol. 211, pp. 345-356, 2018.

[9] W. Verhoef, L. Jia, Q. Xiao, and Z. Su, "Unified optical-thermal four-stream radiative transfer theory for homogeneous vegetation canopies," *IEEE Transactions on geoscience and remote sensing,* vol. 45, no. 6, pp. 1808-1822, 2007.

[10] M. H. Hassoun, *Fundamentals of artificial neural networks*. MIT press, 1995.

[11] J. A. Plascyk and F. C. Gabriel, "The Fraunhofer line discriminator MKII-an airborne instrument for precise and standardized ecological luminescence measurement," *IEEE Transactions on Instrumentation and measurement,* vol. 24, no. 4, pp. 306-313, 1975.

[12] G. A. Carter, "Ratios of leaf reflectances in narrow wavebands as indicators of plant stress," *Remote sensing,* vol. 15, no. 3, pp. 697-703, 1994.